Energies **2015**, *8*, 6286-6301; doi:10.3390/en8076286

OPEN ACCESS

energies

ISSN 1996-1073

www.mdpi.com/journal/energies

Article

Effects of Yaw Error on Wind Turbine Running Characteristics Based on the Equivalent Wind Speed Model

Shuting Wan [1,*], Lifeng Cheng [1,*] and Xiaoling Sheng [1,2]

[1] School of Energy Power and Mechanical Engineering, North China Electric Power University, Baoding 071003, China; E-Mail: sssxlyc@163.com

[2] Department of Electrical Engineering, North China Electric Power University, Baoding 071003, China

* Authors to whom correspondence should be addressed;
E-Mails: 13582996591@139.com (S.W.); clf2001_0@163.com (L.C.);
Tel.: +86-135-8299-6591 (S.W.); +86-158-3225-2609 (L.C.); Fax: +86-312-752-5027 (L.C.).

Academic Editor: Chi-Ming Lai

Received: 8 April 2015 / Accepted: 17 June 2015 / Published: 25 June 2015

Abstract: Natural wind is stochastic, being characterized by its speed and direction which change randomly and frequently. Because of the certain lag in control systems and the yaw body itself, wind turbines cannot be accurately aligned toward the wind direction when the wind speed and wind direction change frequently. Thus, wind turbines often suffer from a series of engineering issues during operation, including frequent yaw, vibration overruns and downtime. This paper aims to study the effects of yaw error on wind turbine running characteristics at different wind speeds and control stages by establishing a wind turbine model, yaw error model and the equivalent wind speed model that includes the wind shear and tower shadow effects. Formulas for the relevant effect coefficients T_c, S_c and P_c were derived. The simulation results indicate that the effects of the aerodynamic torque, rotor speed and power output due to yaw error at different running stages are different and that the effect rules for each coefficient are not identical when the yaw error varies. These results may provide theoretical support for optimizing the yaw control strategies for each stage to increase the running stability of wind turbines and the utilization rate of wind energy.

Keywords: wind turbine; yaw error; running characteristics; equivalent wind speed model

---

1. Introduction

Wind energy has attracted worldwide attention because of its advantages, including the fact that it is a clean form of energy, it has an extremely large energy reserve, its wide availability and its renewability. However, the attributes of natural wind (including wind speed and direction) vary randomly and intermittently. These variations account for the greatest problems associated with developing wind energy. The wind direction changes frequently and randomly relative to the rotor axis of horizontal-axis wind turbines. To improve the utilization of wind energy and optimize the wind loads on the blades, the problems caused by steady-state and transient-state yaw error must be considered. Specific control strategies should be used for wind turbines, including pitch control and generator torque control to respond to wind aped fluctuations as well as active yaw control to cope with frequent changes in wind direction [1,2].

Yaw systems are a very important component of wind turbines. As the wind direction changes, yaw systems stop and start frequently to keep the wind turbine aligned with the wind direction. Under normal operating conditions, the rotor torque fluctuations during yawing and the resistance torque variation in response to changes in the yaw angle and/or wind speed generate load fluctuations in the yaw system [3,4]. These load fluctuations result in further speed fluctuations in the yaw system, which affects the vibrations of the blades, tower and nacelle and even threatens the safety of the wind turbine. With the development of large-scale wind turbines in recent years, stricter requirements for the stability of yaw systems have been proposed, and new opportunities for studying the yaw control systems have been provided. Therefore, an examination of the effects of yaw error on wind turbine running characteristics is crucial to guarantee the secure running status of a wind turbine and improve the efficiency of power generation with great practical value.

Many scholars have studied control strategies for yaw systems. Early wind turbines mainly adopted the Hill Climbing Control (HCC) method for activating yaw, which is limited by wind measurement technology [5–7]. However, the HCC method is no longer applicable for modern large-scale grid-connected wind turbines. With the development of wind sensors, the measurement accuracies of wind vanes and anemometers have increased. Consequently, all modern wind turbines employ active yaw control strategies to keep the turbines facing into the wind by acquiring signals from wind sensors. In Ref. [8] the authors suggested using DSP control and a stepping motor to drive the yaw system and tracking the wind direction automatically. Using this method, the yaw system can quickly and precisely track the wind direction. In Ref. [9], the authors studied the vibration responses of a commercial 2.3 MW turbine to yaw motion and suggested that the analysis of vibration response should be integrated into routines to reduce the downtime and failure frequency of large-scale wind turbines. All of these studies have focused on how to improve the accuracy of the alignment of the yaw system toward the wind direction and have not considered the negative effects resulting from frequent yaw changes. In Ref. [10], a beam model that included geometric nonlinearity coupled with unsteady aerodynamics and based on blade element theory was established. In addition, these authors conducted an aeroelastic analysis under yaw flow conditions and investigated the effects of yaw error on blade behavior and dynamic stability. In Ref. [11], TurbSim, AeroDyn and FAST were used to simulate the aerodynamic and mechanical aspects of a wind turbine. In addition, the effects of yaw error, tower shadow, wind shear and turbulence on the power quality of a wind-diesel system were studied.

In Ref. [12], the alleviation of the blade load variations induced by the wind shear through yaw error is assessed using 3-dimensional geometry. These authors found that the optimal yaw error angles for minimizing the blade load variations could be identified for both deterministic and turbulent inflows. Overall, these authors studied the dynamic characteristics or the power quality of wind turbines under the influence of wind shear, tower shadow or yaw error but did not discuss how these factors affected the wind turbine running characteristics.

Comprehensive statistical data regarding the failure rate and downtime of wind turbines showed that the portion of downtime caused by yaw failures comprised 13.3% of the total downtime [13], while the yaw system failure rate comprised 12.5% [14]. Therefore, the yaw system has a high failure rate, and is time-consuming and difficult to repair once broken [13–17]. If the wind turbine cannot be accurately aligned toward the wind direction because of yaw error or failure, the conditions of the rotor load become worse and the power generation efficiency is reduced or threatens the safe operation of the wind turbine.

This study is based on an established wind turbine, yaw error and equivalent wind speed model that includes wind shear and tower shadow effects [18–21]. Herein, the effects of complex wind conditions on the running characteristics of wind turbines, such as aerodynamic torque, rotor speed and output power, are investigated. The formulas with the relevant effect coefficients T_c, S_c, P_c are derived and the effect rules for each coefficient are studied. A simulation model of a 2.5 MW direct drive wind turbine is presented to support the relevant calculations and analyses.

2. Wind Turbine System Model Description

A complete wind turbine system model with PMSG consists of a wind speed model, rotor model, drive train model, control system, an inverter and transformer model, *etc*. The PMSG is connected to the AC grid by two full back-to-back converters. The layout of the wind turbine system model is depicted in Figure 1.

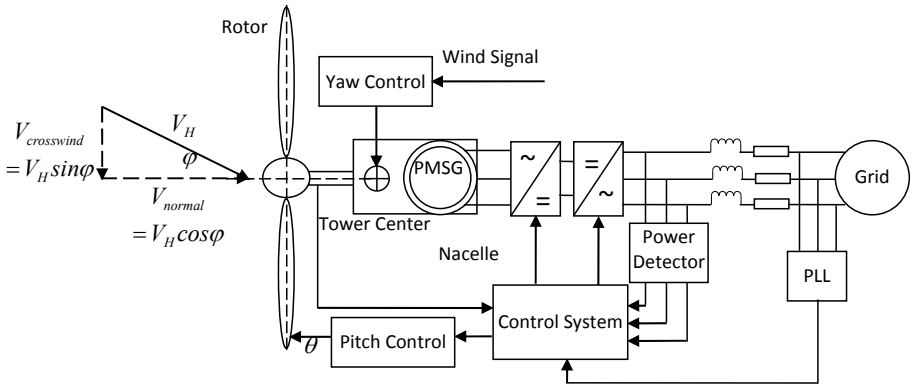

Figure 1. Permanent-magnet direct-drive synchronous wind turbine system model.

2.1. Equivalent Wind Speed Model

The equivalent wind speed model, which was first proposed by Dale in Ref. [21], considers the effects of wind shear and tower shadow. Wind shear refers to increases in the wind speed with height due to friction between the Earth's surface and the wind. Tower shadow effect refers to

the reduction in the air flow due to the presence of the tower. For three-bladed wind turbine, the rotor aerodynamic torque exists 3P (3 is the number of blades, P is the rotor rotation angular frequency) ripple component caused by the wind shear and tower shadow. Thus, this model can more accurately reflect the wind load conditions of the wind turbine. The equivalent wind speed analytical equations are derived in the paper and introduced here briefly.

Based on this model, the equivalent wind speed over the rotor area v_{eq} consists of three components: The wind speed at hub height v_{eq_0}, the wind shear component $v_{eq_{ws}}$ and the tower shadow component $v_{eq_{ts}}$. The equivalent wind speed and its analytical equations are shown in Equations (1)–(6):

$$v_{eq} = v_{eq_0} + v_{eq_{ws}} + v_{eq_{ts}} \tag{1}$$

$$v_{eq_0} = V_H \tag{2}$$

$$v_{eq_{ws}} = V_H \cdot \left[\frac{\alpha(\alpha-1)}{8}\left(\frac{R}{H}\right)^2 + \frac{\alpha(\alpha-1)(\alpha-2)}{60}\left(\frac{R}{H}\right)^3 \cos 3\beta \right] \tag{3}$$

$$v_{eq_{ts}} = \frac{MV_H}{3R^2} \cdot \sum_1^3 \left[\frac{a^2}{\sin^2\beta_b} \ln\left(\frac{R^2\sin^2\beta_b}{x^2} + 1 \right) - \frac{2a^2R^2}{R^2\sin^2\beta_b + x^2} \right] \tag{4}$$

$$\beta_1 = \beta \qquad \beta_2 = \beta + \frac{2\pi}{3} \qquad \beta_3 = \beta + \frac{4\pi}{3} \tag{5}$$

$$V_0 = \left[1 + \frac{\alpha(\alpha-1)R^2}{8H^2} \right] V_H = M \cdot V_H \tag{6}$$

where V_H is the wind speed at the height of hub center (m/s); α is the wind shear exponent, its empirical value is affected by the surface roughness (Table 1); H is the height of the hub center (m); β is the blade azimuth angle (°) and varies from 0°–360°; β_b is the blade azimuth angle of each blade (°), which varies from 0°–360°, and can be defined by Equation (5) for the three-blades wind turbines; a is the tower radius (m); x is the distance from the tower midline to the blade (m), as shown in Figure 2; V_0 is the mean wind speed; and M is the wind speed conversion factor.

Table 1. Variation of α empirical values with terrain.

Terrain	α
Smooth (Sea, Sand, Snow, *etc.*)	0.10–0.13
Medium irregularities (Prairie, Farmland, Villages, *etc.*)	0.13–0.20
Irregularities (Forests, Suburbs, *etc.*)	0.20–0.27
Very irregularities (City, Tall buildings, Hills, *etc.*)	0.27–0.40

2.2. Wind Turbine Model

Using aerodynamics, a simplified mathematical model can be created for the wind turbine based on the aerodynamic power and torque, as shown in Equations (7)–(9):

$$P_w = \frac{1}{2}\rho\pi R^2 v_{eq}^3 C_p(\theta,\lambda) \tag{7}$$

$$T_w = \frac{1}{2}\rho\pi R^3 v_{eq}^2 \frac{C_p(\theta,\lambda)}{\lambda} \tag{8}$$

$$\lambda = \frac{\omega_r R}{v_{eq}} \tag{9}$$

The relationship between P_w and T_w is as follows:

$$P_w = T_w \cdot \omega_r \tag{10}$$

where P_w is the wind turbine output power (W); T_w is the rotor aerodynamic torque (Nm); ρ is the air density (kg/m^3); R is the rotor radius (m); θ is the blade pitch angle (°); λ is the tip-speed ratio; $C_p(\theta, \lambda)$ is the rotor power coefficient; and ω_r is the rotor angular speed (rad/s). Figure 2 shows the definition of some dimensional parameters of the wind turbine.

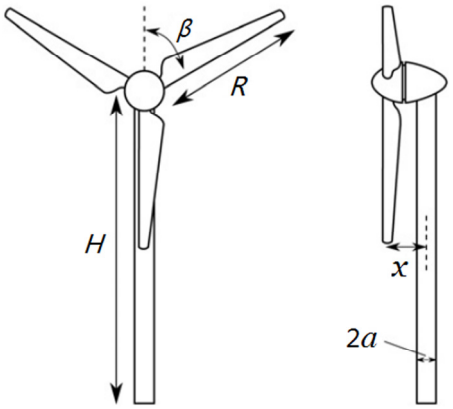

Figure 2. Definition of some dimensional parameters of the wind turbine.

This model may be overly simplistic for assessing dynamic loads in a meaningful way, but because the equivalent wind speed model clearly relies on many wind turbine dimensional parameters such as H, R, x, a and a time-dependent parameter β. This model is useful for the real-time analysis of wind turbine simulators.

2.3. Yaw Error Model

The wind sensor installed on the top of the wind turbine consists of two parts, the anemometer and the wind vane. The anemometer is used to measure the wind speed and sends real time signals to the control system for power regulation. The wind vane is used to measure the wind direction and was used to control the yawing according to an established yaw control strategy after it was processed by the yaw control system. All modern wind turbine yaw systems are required to have certain inertias to ensure operational stability and to keep the current state within a certain range over a certain period during the mean wind direction changes.

At the onset of a change in wind direction or of a yaw alignment delay, an angle is formed between the wind direction and the rotor axis. This angle is called the yaw error and is depicted in Figure 1. Because natural wind is very random, with rapid and frequent changes in wind speed and wind direction, wind turbines are most often operating under the yaw error state.

In the yaw error model, the wind can be decomposed into the two following components:

$$V_{\text{normal}} = V_{\text{H}}\cos\varphi \tag{11}$$

$$V_{\text{crosswind}} = V_{\text{H}}\sin\varphi \tag{12}$$

Here, V_{normal} is the effective component in the opposite direction of the rotor axis and ensures that the wind turbine is operating normally. Meanwhile, $V_{\text{crosswind}}$ is the lateral component, referred to as the cross wind component, which does not have an effect on normal operation of the wind turbine but only produces lateral loads. Variations in wind speed and/or a sudden change in wind direction will change both of these two components [22], which will affect the wind loads and wind turbine running characteristics.

3. Wind Turbine Running Characteristics Simulation Analysis

3.1. Simulation Parameters

This paper considers a 2.5 MW permanent-magnet direct-drive synchronous wind turbine located on a wind farm in southern China as an example for data acquisition and simulation analysis. The wind turbine is located in the plateau and hilly area on an S-type wind farm, where the air density is low. On the wind farm, vegetation growth is very prosperous, and the terrain is rolling. Consequently, the wind shear exponent is large. Thus, the wind speed and wind direction change frequently due to the climate and terrain or other factors. The parameters of the wind turbine and wind farm are shown in Table 2.

Table 2. Parameters of the 2.5 MW permanent-magnet direct-drive synchronous wind turbine.

Parameters of the Wind Turbine	Value
Blades	3
Rotor diameter	113 m
Rated power	2500 kW
Cut-in wind speed	3 m/s
Cut-out wind speed	22 m/s
Rated wind speed	10.5 m/s
Mean wind speed for the wind farm	7 m/s
Maximum rotor power coefficient	0.500422
Optimal tip speed ratio	8.7
Rated speed	13 r/min
Center height of the hub	87 m
Tower(conical) outside diameter	4630/3040 mm
Minimum distance from the tip to the tower	5.2 m
Rated torque	2010 kNm
Air density	1.065 kg/m^3
Wind shear exponent	0.4

The wind turbine control strategy can be divided into three stages according to the wind speed: Below the rated speed, below the rated power and constant rated power. In the below rated speed stage, the wind turbine operates at the optimal tip speed ratio and achieves the maximum rotor power

coefficient. The rotor speed matches the changes in the wind speed by adjusting the generator torque. In the below rated power stage, the rotor speed has already reached the rated speed and remains constant; however, the output power is less than the rated power. In addition, the rotor aerodynamic torque matches the changes in the wind speed in this stage by adjusting the generator torque while using the rotor speed as a control parameter. In the constant rated power stage, the wind speed is sufficiently strong for the wind turbine to run at its rated power and the generator torque to remain at the rated torque. In this stage, the pitch angle is adjusted to match the rotor aerodynamic torque to the generator torque. In different stages, the wind turbine running characteristics and the control parameters are different. In this paper, the effects of yaw error on running characteristics are determined during different stages.

3.2. Analysis of the Effects of Yaw Error on Rotor Torque

As discussed above, in the below rated speed and below rated power stages, the wind turbine is controlled by adjusting the generator torque. However, in the constant rated power stage, the wind turbine is controlled by adjusting the aerodynamic torque captured from the wind to match the generator torque. Therefore, the torque ripple has very important effects on the operation and control of the wind turbine. According to the equivalent wind speed model and the yaw error model, the rotor aerodynamic torque can be expressed as follows:

$$T_{\mathrm{t}}(\beta,\varphi) = T_0\left[1+2\frac{1-m}{m}+\frac{2}{v_0}(v_{\mathrm{eq_{ts}}}+v_{\mathrm{eq_{ws}}})\right]\cos^2\varphi \tag{13}$$

$$T_0 = \frac{1}{2}\rho\pi R^3 V_{\mathrm{H}}^2\frac{C_{\mathrm{p,max}}}{\lambda_{\mathrm{opt}}} \tag{14}$$

$$T_{\mathrm{c}} = \left[1+2\frac{1-M}{M}+\frac{2}{MV_{\mathrm{H}}}(v_{\mathrm{eq_{ts}}}+v_{\mathrm{eq_{ws}}})\right]\cos^2\varphi \tag{15}$$

Equation (13) shows that the rotor aerodynamic torque is a function of the blade azimuth angle β and yaw error angle φ. β undergoes periodic variations as the rotor rotates and can be converted into a temporal parameter such that the rotor aerodynamic torque also varies periodically with time. The ideal constant torque T_0 results from the mean wind speed without considering the wind shear, tower shadow and yaw error, and T_{c} is the total aerodynamic torque coefficient.

The effects of wind shear and tower shadow on the aerodynamic torque coefficient are shown in Figure 3. A 3P pulsation in the aerodynamic torque is clearly observed. The effect on the torque ripple of wind shear alone is approximately 0.7%, that of tower shadow alone is approximately 9%, and the total effect is approximately 10%. A similar conclusion was also obtained in Ref. [21].

Figure 4 shows the effects on the total aerodynamic torque coefficient of the yaw error based on the equivalent wind speed model. Table 3 presents the values of the total aerodynamic torque coefficient oscillations. It is observed that, the ripple of the total aerodynamic torque coefficient differs significantly by the azimuth angle of the rotor. When the blade is not in the tower shadow zone, the ripple of the total aerodynamic torque coefficient due to the yaw error is very small. In addition, the yaw error angles negatively affect the torque coefficient because the torque coefficient decreases as

the yaw error angle increases, which is subtle. When the blade is in the tower shadow zone, the yaw error angle positively affects the torque coefficient, and the torque coefficient increases as the yaw error angle increases. The yaw error angle can restrain the ripple of the torque coefficient. As the yaw error angle increases, the restraining effect becomes significantly stronger. Although the existence of the yaw error can restrain the ripple of the torque coefficient, the effect of the yaw error on the total aerodynamic torque increases markedly as the yaw error angle increases.

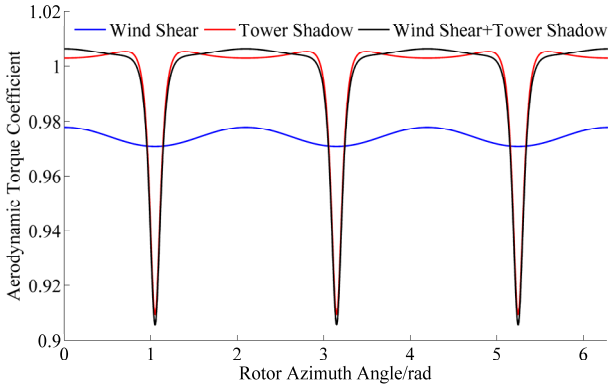

Figure 3. Effects of wind shear and tower shadow on the aerodynamic torque coefficient.

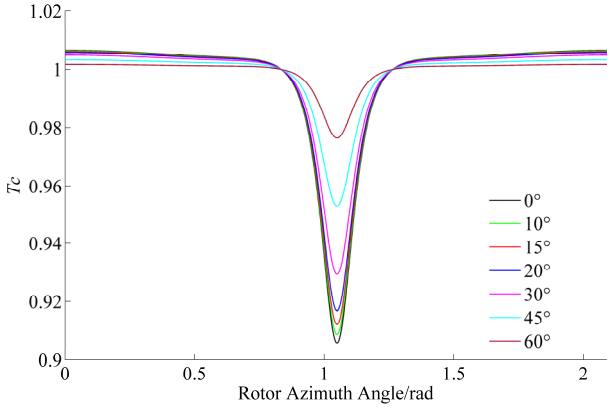

Figure 4. Variation in T_c due to yaw error.

Table 3. T_c oscillation values.

Yaw Error	Blade not in the Tower Shadow Zone	Blade in the Tower Shadow Zone
0°	0.0065	−0.0960
10°	0.0062	−0.0938
15°	0.0060	−0.0892
20°	0.0056	−0.0845
30°	0.0049	−0.0718
45°	0.0031	−0.0479
60°	0.0015	−0.0240

Furthermore, as shown in Equation (13), when the yaw error is 10°, the torque ripple is approximately 3%, and when the yaw error is 15°, the torque ripple is approximately 6.7%, which is slightly smaller than the effect on the torque ripple of the tower shadow alone. All these effects are

within an acceptable range for normal operation. However, when the yaw error is larger (e.g., 30°, 45° or 60°), the torque loss is very large, and the loss rates are all greater than 25%, which strongly affects the normal operation of the wind turbine.

3.3. Analysis of the Effects of Yaw Error on Rotor Speed

As shown in Figure 5, the permanent-magnet direct-drive synchronous wind turbine speed control strategy can be divided into four stages: I, Startup with a constant rotor speed; II, Increasing rotor speed with increasing wind speed; III, Constant rated speed with a moderate wind speed; and IV, Constant rated speed with a high wind speed. Stage I is the start of the wind turbine, and the wind is low and varies over a narrow range; as a result, the running state of the wind turbine quickly transitions to stage II after entering stage I. Therefore, stage I is not described in this paper.

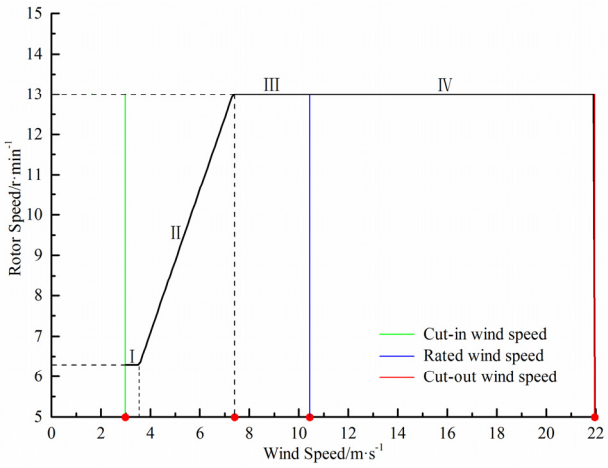

Figure 5. Rotor speed control.

Similar to the rotor torque derivation and according to the equivalent wind speed model and the yaw error model, the rotor speed can be expressed as follows:

$$\omega_t(\beta,\varphi) = \omega_0 \frac{1}{M}\left[1+\frac{1}{V_H}(v_{eq_{ts}}+v_{eq_{ws}})\right]\cos\varphi = \omega_0 \cdot S_c \tag{16}$$

$$\omega_0 = \frac{\lambda_{opt} V_H}{R} \tag{17}$$

$$S_c = \frac{1}{M}\left[1+\frac{1}{V_H}(v_{eq_{ts}}+v_{eq_{ws}})\right]\cos\varphi \tag{18}$$

Equation (16) shows that the rotor speed, $\omega_t(\beta,\varphi)$, is a function of the blade azimuth angle, β, and the yaw error angle, φ. The ideal constant torque, ω_0, results from the mean wind speed and does not consider the wind shear, tower shadow and yaw error. S_c is the rotor speed coefficient.

At different stages, the effects of yaw error on rotor speed at different wind speeds are shown in Figure 6 and Table 4. In stage II, the wind speed is lower than 7.4 m/s and the rotor speed has not reached the rated speed. In this stage, the tip speed ratio will remain at the optimum value. As shown in Figure 6a, the wind speed V_H = 7 m/s, when the yaw error is 10°, the rotor speed loss is

approximately 1.44%, when the yaw error is 15°, the rotor speed loss is approximately 3.35%, and when the yaw error is 30°, the rotor speed loss reaches approximately 12.92%.

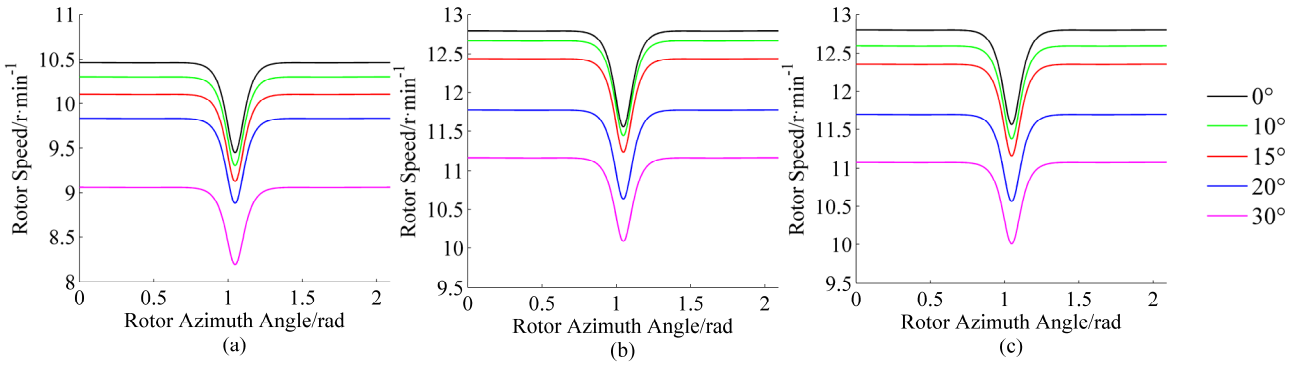

Figure 6. Effects of yaw error on rotor speed by stage: (**a**) Stage II, V_H = 7 m/s. (**b**) Stage III, V_H = 10 m/s. (**c**) Stage IV, V_H = 15 m/s.

Table 4. Values of rotor speed oscillation.

Yaw Error	V_H = 7 m/s		V_H = 10 m/s		V_H = 15 m/s	
	Rotor Speed	Speed Loss	Rotor Speed	Speed Loss	Rotor Speed	Speed Loss
0°	10.45	0	12.80	0	12.80	0
10°	10.30	1.44%	12.70	0.78%	12.60	1.56%
15°	10.10	3.35%	12.45	2.73%	12.35	3.52%
20°	9.80	6.22%	11.80	7.81%	11.70	8.60%
30°	9.10	12.92%	11.20	12.50%	11.10	13.30%

In stage III, the wind speed is between 7.4 m/s and 10.5 m/s and the rotor speed has reached the rated speed, but the wind turbine power has not yet reached the rated power. To maintain the turbine at a constant rated speed, the tip speed ratio decreases as the wind speed increases. As observed in Figure 6b, the wind speed is V_H = 10 m/s, when the yaw error is 10°, the rotor speed loss is approximately 0.78%, when the yaw error is 15°, the rotor speed loss is approximately 2.73%, and when the yaw error is 30°, the rotor speed loss reaches approximately 12.50%.

In stage IV, the wind speed is higher than 10.5 m/s, the rotor speed has reached the rated speed, and the wind turbine power has reached the rated power. As shown in Figure 6c, for a wind speed of V_H = 15 m/s, when the yaw error is 10°, the rotor speed loss is approximately 1.56%, when the yaw error is 15°, the rotor speed loss is approximately 3.52%, and when the yaw error is 30°, the rotor speed loss reaches approximately 13.30%.

Comparing the simulation results presented in Figure 6, it can be concluded that, the yaw error has little effect on the rotor speed ripple but can restrain the torque oscillation. In addition, the effects of a given yaw error on rotor speed differ for different stages. These effects are most prominent in stage IV, followed by stage II, and are the weakest in stage III. Furthermore, compared with the rotor speed ripple amplitude caused by wind shear and tower shadow, the rotor speed variation caused by a yaw error within 15° is very small (no more than 1/3) and the variation caused by a yaw error of 20° or more is comparable to the wind shear and tower shadow.

Figure 7 shows the effects of yaw error on the rotor speed coefficient obtained from the simulation results. When the rotor is at various azimuth angles, the rotor speed coefficient also includes 3P ripple components. When the blade is not in the tower shadow zone, the rotor speed coefficient remains nearly constant value. However, when the blade is in the tower shadow zone, the rotor speed coefficient significantly oscillates around a value of approximately 0.05. This effect results from the wind shear and, in particular, the tower shadow. The S_c oscillation values are shown in Table 5. When the yaw error is 10°, the attenuation of the rotor speed coefficient is approximately 0.011, and when the yaw error is 20°, the attenuation is approximately 0.058, which is nearly equal to the ripple values resulting from the wind shear and tower shadow. In addition, the oscillation value of the rotor speed coefficient is only weakly affected by the yaw error.

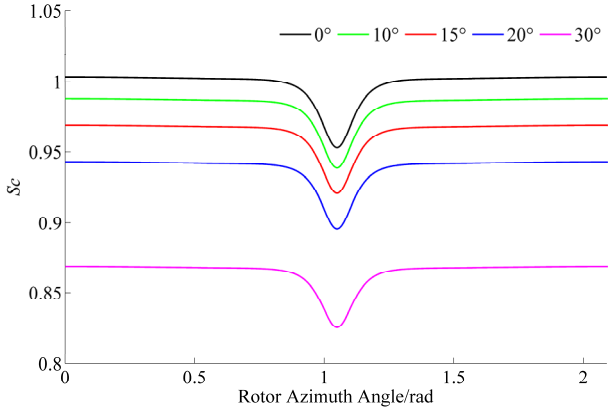

Figure 7. Effects of yaw error on S_c.

Table 5. Values of S_c oscillation.

Yaw Error	Oscillation Value	Reduce Value
0°	0.051	0
10°	0.053	0.011
15°	0.050	0.031
20°	0.049	0.058
30°	0.045	0.133

3.4. Analysis of the Effects of Yaw Error on Wind Turbine Power

Here, we substitute Equations (13) and (16) into Equation (10) to obtain a final expression for the effects of yaw error on the wind turbine power:

$$P_w(\beta,\varphi) = T_w(\beta,\varphi)\cdot\omega_t(\beta,\varphi) = T_0\omega_0 T_c S_c \tag{19}$$

$$P_c = T_c \cdot S_c \tag{20}$$

where P_c is the wind turbine power coefficient, T_c is the total aerodynamic torque coefficient, and S_c is the rotor speed coefficient. Figure 8 shows the effect curves of for the effect of yaw error on the wind turbine power coefficient.

Figure 8 shows that 3P ripple components are present in P_c (the synthesis of T_c and S_c) as well, and the oscillation significantly affected by the yaw error, as shown in Table 6. The yaw error angle can

restrain the oscillation of P_c, and this restrain effect becomes stronger as the yaw error angle increases. This result is similar to the effects of yaw error on T_c. Meanwhile, P_c is reduced by a factor of cos φ. In Ref. [23], the experimental results suggest that the power output is reduced by a factor of $\cos^2$ φ, and in Ref. [1], the relationship between the power output and the yaw error follows the cosine-cubed law $P_{yaw} = P_w\cos^3$ φ, which results from a simplified analysis of the yawed performance without considering adjustments to the control parameters, such as θ, λ, C_p, and T_e (generator electromagnetic torque).

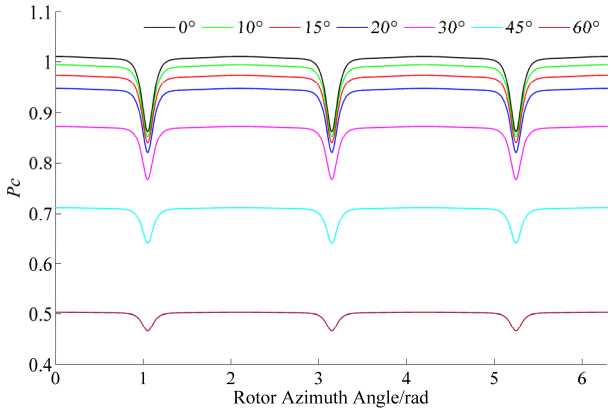

Figure 8. Effects of yaw error on P_c.

Table 6. Values of P_c oscillation.

Yaw Error	Oscillation Value	Reduce Value
0°	0.148	0
10°	0.141	0.015
15°	0.134	0.034
20°	0.128	0.061
30°	0.107	0.137
45°	0.072	0.298
60°	0.038	0.507

Figure 9 depicts the effects of yaw error on the wind turbine power obtained from the simulation results and also shows that the effects of yaw error on power loss vary markedly by wind speed stages.

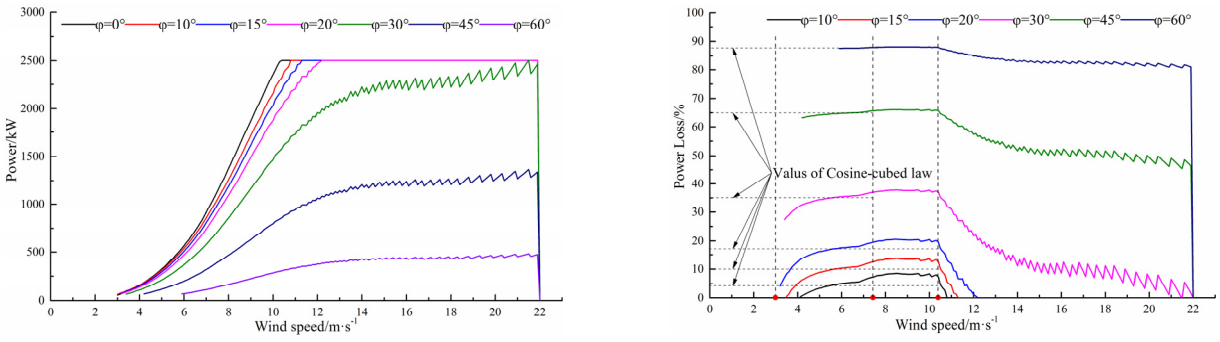

(**a**) (**b**)

Figure 9. Effects of yaw error on the wind turbine power. (**a**) Wind turbine power curve; (**b**) Power loss curve.

When the wind speed is less than 7.4 m/s, the wind turbine is in the below rated speed stage. In this stage, the wind turbine runs at the optimal tip speed ratio, and the maximum rotor power coefficient is achieved. Figure 9b shows that the effect of yaw error on the power loss gradually increases with the wind speed. When the yaw error angle is small (e.g., 10°, 15° and 20°), the power loss curve rapidly approaches and even exceeds the cosine-cubed law values. When the yaw error angle is large (e.g., 30°, 45° and 60°), the power loss curve is approximately linearly close to the cosine-cubed law values as the limits.

When the wind speed varies between 7.4 m/s and 10.5 m/s, the wind turbine operates in the below rated power stage. In this stage, the pitch angle is still 0°, and the tip speed ratio and the rotor power coefficient both decrease slowly as the wind speed increases. The effects of yaw error on the wind turbine power are generally stable, and the power loss rate reaches a maximum and ceases to change with variations in the wind speed. At this stage, the large yaw error angle agrees well with the value of the cosine-cubed law. However, regarding small yaw error angles, the wind turbine power loss reaches approximately 8% for a yaw error angle of 10° and approximately 13% for a yaw error angle of 15°. Both of these values are much higher than the values of 4.5% and 9.9% predicted by the cosine-cubed law.

When the wind speed is greater than 10.5 m/s, the wind turbine operates in the constant rated power stage. The pitch angle increase is controlled to adjust the wind turbines to capture the aerodynamic torque. The rotor power coefficient rapidly decreases as the wind speed increases. This control strategy ensures that the wind turbine runs at the rated power and protects the turbine from damage due to excessive wind loads. The effects of yaw error on wind turbine power begin to differentiation, and Figure 9 shows the differentiation that, the effect of yaw error decreases rapidly to zero when the yaw error is small (e.g., 10°, 15° and 20°), the wind turbine can quickly reach the rated power; nevertheless, the wind turbine can no longer reach the rated power when the yaw error is large (e.g., 30°, 45° and 60°), leading to wasted wind energy.

According to the above analysis, the effects of yaw error on the power output and power coefficient differ by case, and the effects do not follow the $\cos^2 \varphi$ law in Ref. [23] or the $\cos^3 \varphi$ law in Ref. [1].

4. Discussion

Based on the simulation results presented in Section 3, the effects of yaw error on the wind turbine running characteristics during different wind speed stages are obviously different. First, when the rotor is at different azimuth angles, the effects of the wind shear, tower shadow and yaw error on T_c differ. Although the wind shear and tower shadow result in T_c 3P pulsation, the yaw error can restrain the 3P pulsation. In addition, as the yaw error increases, the restraining effect becomes more significant. Second, the wind shear and tower shadow also lead to rotor speed 3P pulsation. However, in contrast with the case of T_c, the yaw error has nearly no restraining effect on the S_c 3P pulsation, it only decreasing the rotor speed and S_c. Furthermore, the effects of a given yaw error on rotor speed are significantly different for different wind speed stages. Third, the yaw error angle can restrain the P_c oscillation and reduce the value of P_c by a factor of $\cos \varphi$. However, the effects of yaw error on the power loss are more complicated because the effect rules do not follow the $\cos^2 \varphi$ law or the $\cos^3 \varphi$ law. Consequently, there are significant differences between the running stages.

The formulation of a wind turbine control strategy that includes the yaw control strategy must be based on the mechanical properties of normal operation and consider the factors of power loss, rotor torque and speed ripple, as well as the running characteristics of the wind turbine system and the response speeds of the subsystems. Based on this paper, a yaw control strategy can be formulated for different stages, and each stage can be used to set a different yaw error control precision, execution times and response speeds to more effectively reduce the yaw frequency and failure rate of yaw systems.

In spite of this, the models we used are low-order models after all, the discussions above are useful to provide theoretical support for optimizing yaw control strategy in stages, but it is difficult to assess the highly yawed flow in industrial practice. Because of the complex phenomena that vortices and stall become more and more important in high misalignment cases, high-order models are requested to accurate calculation and analysis in dynamic load, power assessment *etc.*

5. Conclusions

In this paper, equivalent wind speed, wind turbine and yaw error models have been described and established. Using Matlab for simulation calculation and based on an analysis of the simulation results, the effects of yaw error on the running characteristics in different running stages were studied. The calculation formulas of relevant effect coefficients T_c, S_c and P_c were derived. These results reveal that the effects of yaw error on aerodynamic torque, rotor speed and power output are significantly different and can be divided into several stages according to the wind speed. Thus, this paper contributes to a better understanding of the details of the effects of yaw error on the running characteristics, and further studies regarding these details should be conducted to provide a reference for optimizing the yaw control strategy in stages.

Acknowledgments

The research was supported by the Fundamental Research Funds for the Central Universities No. 12MS101 and 2014XS82. The authors are grateful for this support.

Author Contributions

Shuting Wan contributed to the numerical tool validations and the original data acquisition from wind farm. Lifeng Cheng contributed to the numerical simulations, analysis and interpretations, writing and editing including the overall idea of the manuscript. Xiaoling Sheng contributed to the original data extraction and analysis.

Conflicts of Interest

The authors declare no conflict of interest.

References

1. Burton, T.; Jenkins, N.; Sharpe, D.; Bossanyi, E. *Wind Energy Handbook*, 2nd ed.; John Wiley & Sons Ltd.: Chichester, UK, 2011.

2. Jelavic, M.; Petrovic, V.; Peric, N. Estimation based individual pitch control of wind turbine. *AUTOMATIKA J. Control Meas. Electron. Comput. Commun.* **2010**, *51*, 181–192.
3. Ekelund, T. Yaw control for reduction of structural dynamic loads in wind turbines. *J. Wind Eng. Ind. Aerodyn.* **2000**, *85*, 241–262.
4. Ekelund, T. Dynamics and control of structural loads of wind turbines. In Proceedings of the American Control Conference, Philadelphia, PA, USA, 21–26 June 1998; Volume 3, pp. 1720–1724.
5. Farret, F.A.; Pfitscher, L.L.; Bernardon, D.P. Sensorless active yaw control for wind turbines. In Proceedings of the 27th Annual Conference of the IEEE Industrial Electronics Society, Denver, CO, USA, 29 November–2 December 2001; Volume 2, pp. 1370–1375.
6. Farret, F.A.; Pfitscher, L.L.; Bernardon, D.P. Active yaw control with sensorless wind speed and direction measurements for horizontal axis wind turbines. In Proceedings of the 2000 Third IEEE International Caracas Conference on Devices, Circuits and Systems, Cancun, Mexico, 15–17 March 2000; Volume 25, pp. 1–6.
7. Farret, F.A.; Pfitscher, L.L.; Bernardon, D.P. A heuristic algorithm for sensorless power maximization applied to small asynchronous wind turbogenerators. In Proceedings of the 2000 IEEE International Symposium on Industrial Electronics, Cholula, Puebla, Mexico, 4–8 December 2000; Volume 1, pp. 179–184.
8. Bu, F.F.; Huang, W.X.; Hu, Y.W.; Shi, K.; Wang, Q.S. Study and implementation of a control algorithm for wind turbine yaw control system. In Proceedings of the 2009 World Non-Grid-Connected Wind Power and Energy Conference, Nanjing, China, 24–26 September 2009; pp. 1–5.
9. Bassett, K.; Carriveau, R.; Ting, D. Vibration response of a 2.3 MW wind turbine to yaw motion and shut down events. *Wind Energy* **2011**, *14*, 939–952.
10. Jeong, M.S.; Kim, S.W.; Lee, I.; Yoo, Y.J.; Park, Y.C. The impact of yaw error on aeroelastic characteristics of a horizontal axis wind turbine blade. *Renew. Energy* **2013**, *60*, 256–268.
11. Roohollah, F.; Gerry, M.; Mehrdad, M. The impact of tower shadow, yaw error, and wind shears on power quality in a wind-diesel system. *IEEE Trans. Energy Convers.* **2009**, *24*, 102–111.
12. Kragh, K.A.; Hansen, M.H. Load alleviation of wind turbines by yaw misalignment. *Wind Energy* **2014**, *17*, 971–982.
13. Ribrant, J.; Bertling, L. Survey of failures in wind power systems with focus on Swedish wind power plants during 1997–2005. *IEEE Trans. Energy Convers.* **2007**, *22*, 167–173.
14. Cristian, B. Modeling Lifetime of high power IGBTs in wind power applications—An overview. In Proceedings of the IEEE International Symposium on Industrial Electronics, Gdansk, Poland, 27–30 June 2011; pp. 1408–1413.
15. Pinar Pérez, J.M.; García Márquez, F.P.; Tobias, A.; Papaelias, M. Wind turbine reliability analysis. *Renew. Sustain. Energy Rev.* **2013**, *23*, 463–472.
16. Fischer, K.; Besnard, F.; Bertling, L. Reliability Centered Maintenance for wind turbines based on statistical analysis and practical experience. *IEEE Trans. Energy Convers.* **2012**, *27*, 184–195.
17. Guo, H.T.; Watson, S.; Tavner, P.; Xiang, J.P. Reliability analysis for wind turbines with incomplete failure data collected from after the date of initial installation. *Reliab. Eng. Syst. Saf.* **2009**, *94*, 1057–1063.

18. Hughes, F.M.; Anaya-Lara, O.; Ramtharan, G.; Jenkins, N.; Strbac, G. Influence of tower shadow and wind turbulence on the performance of power system stabilizers for DFIG-based wind farms, *IEEE Trans. Energy Convers.* **2008**, *23*, 519–528.
19. Hu, W.H.; Su, C.; Chen, Z. Impact of wind shear and tower shadow effects on power system with large scale wind power penetration. In Proceedings of the 37th Annual Conference on IEEE Industrial Electronics Society, Melbourne, Australia, 7–10 November 2011; pp. 878–883.
20. Tan, J.; Hu, W.H.; Wang, X.R.; Chen, Z. Effect of tower shadow and wind shear in a wind farm on AC Tie-Line power oscillations of interconnected power systems. *Energies* **2013**, *6*, 6352–6372.
21. Dale, S.L.D.; Peter, W.L. Simulation model of wind turbine 3p torque oscillations due to wind shear and tower shadow. *IEEE Trans. Energy Convers.* **2006**, *21*, 717–724.
22. Manwell, J.F.; McGowan, J.G.; Rogers, A.L. *Wind Energy Explained-Theory, Design and Application*, 2nd ed.; John Wiley & Sons Ltd.: Chichester, UK, 2009.
23. Madsen, H.A.; Srensen, N.N.; Schreck, S. Yaw aerodynamics analyzed with three codes in comparison with experiment. In Proceedings of the 41st Aerospace Sciences Meeting and Exhibit, Reno, NV, USA, 6–9 January 2003; pp. 94–103.